Journal of the European Ceramic Society 23 (2003) 345–355

www.elsevier.com/locate/jeurceramsoc

# Dielectric investigations on 'MgAlON' compounds: role of nitrogen content

O. Morey[a], P. Goeuriot[a,*], D. Juve[b], D. Treheux[b]

[a]*ENSMSE, 158 Cours Fauriel, F-42023 Saint-Etienne cedex2, France*
[b]*Ecole Centrale, IFOS, UMR 5621, BP 163, 36 Avenue Guy de Collongue, 69131 Ecully, France*

Received 20 October 2001; received in revised form 28 May 2002; accepted 16 June 2002

**Abstract**

The dielectric properties of dense polycrystalline magnesium aluminium oxynitride have been investigated up to 90 °C. The oxygen/nitrogen substitution on the anionic lattice of this solid solution enhances the charge trapping ability and the dielectric breakdown of 'MgAlON' compounds. Oxygen vacancies, which play the role of electron traps, can partially explain the good dielectric properties of this solid solution at low temperature; but they are ineffective for higher temperature where the charge trapping phenomenon remains active. This behaviour, specific to 'MgAlON' solid solution, is explained on the basis of a crystallographic model of atom repartition: this spinel structure offers rich-nitrogen zones randomly located as $AlN_4$ clusters which generate locally the heterogeneous zones of electric charge supposed to be responsible for the good dielectric performance of 'MgAlON' compounds. The local polarizability is modified which enhances the charge-trapping phenomenon.


*Keywords:* Dielectric breakdown; Dielectric properties; MgAlON

## 1. Introduction

The electrical breakdown strength of ceramic materials is an essential characteristic because of their potential application as electrical insulators. However, the physics of these insulating materials appears to be a complex science that requires basic knowledge of the concept of the polaron. The latter can explain trapping and detrapping phenomena and their consequences from an energetic point of view.[1] The breakdown phenomenon is usually described by a variety of mechanisms: intrinsic breakdown (electronic origin), thermal breakdown (overheating of the material due to Joule effect), avalanche breakdown (initiated by gas discharges in pores).

Our approach in this study was fundamentally different and principally centred on the experimental determination of two intrinsic characteristics of insulators: the breakdown strength and the trapping efficiency. The notion of intrinsic characteristic is questionable while no intrinsic parameters such as sample shape, electrode geometry or frequency form of the applied electrical field can significantly influence the breakdown strength value[2] It is also true that electrical behaviour of 'MgAlON' compounds at room and high temperature has not been published yet.

The effect of porosity on the breakdown strength has been put forward in the first part of the study. The trapping efficiency measurements have been performed exclusively on dense samples where all 'MgAlON' compounds exhibit a similar microstructure. The role of point defects in these materials will be also discussed on the basis of a recent powder crystallographic model of 'MgAlON' solid solution [3,4] and on the basis of spectroscopic techniques such as thermoluminescent measurements.

## 2. Experimental procedure

### 2.1. Sample preparation

Magnesium aluminium oxynitride powders with specific compositions have been previously synthesised by solid state reaction between AlN, MgO and $\alpha$-$Al_2O_3$.

* Corresponding author. Tel.: +33-4-77420019; fax: +33-4-77420249.
*E-mail address:* pgoeurio@emse.fr (P. Goeuriot).

0955-2219/02/$ - see front matter 
PII: S0955-2219(02)00195-4

Table 1
Studied compositions

| Compounds | Formulation | $a$ (nm) |
|---|---|---|
| A | $Mg_{0.726}Al_{2.222}O_{3.883}N_{0.117}$ | 0.8044 |
| B | $Mg_{0.538}Al_{2.419}O_{3.667}N_{0.333}$ | 0.8026 |
| C | $Mg_{0.374}Al_{2.551}O_{3.598}N_{0.402}$ | 0.7993 |

Table 2
Densification rate for all samples

| | A | B | C | S30Cr |
|---|---|---|---|---|
| 1650 °C—5 h | 75.7 | 68.9 | 68.3 | 94.1 |
| 1650 °C—11 h | 77.6 | 75.1 | 69.9 | 95.0 |
| 1750 °C—2 h | 95.7 | 94.7 | 94.4 | 95.2 |
| 1750 °C—8 h | 97.8±0.1 | 97.7±0.1 | 97.6±0.1 | 95.5±0.1 |
| 1750 °C—14 h | 98.4±0.1 | 98.3±0.1 | 97.8±0.1 | 95.8±0.2 |
| 1850 °C—5 h | 98.6±0.1 | 98.5±0.1 | 98.1±0.1 | 96.0±0.1 |
| 1850 °C—11 h | 99.0±0.1 | 98.6±0.1 | 98.2±0.1 | 95.2±0.1 |
| 1650 °C—0 h | 59.6 | 57.6 | 56.7 | 92.6 |
| 1750 °C—0 h | 75.3 | 72.7 | 69.8 | 94.1 |
| 1850 °C—0 h | 96.7 | 97.5 | 96.5 | 94.7 |

More information about the synthesis conditions leading to 'MgAlON' compounds has been recently reported.[3,5] Three single-phase compositions denoted A, B, C have been retained for this study. Chemical analyses and XRD patterns determine their stoichiometry, lattice parameter and impurity content. The formulation of the studied compositions is listed in Table 1.

The three powders exhibit a mean crystalline size of approximately 500 nm and a bimodal distribution indicating that the particles are agglomerated and composed of several cristallites. The BET surface area varies from 4.2 to 5.8 $m^2/g$ the A–C compounds.

Moreover a commercial magnesium aluminate $MgAl_2O_4$ powder labelled S30Cr provided by Baïkowski (France) is chosen for its composition which is closed to the ideal stoichiometry, the dielectric behaviour of this sample will be considered as a reference for the nitrogen influence on the dielectric properties of 'MgAlON' compounds. The main difference between the A–C powders is a greater content of nitrogen. The impurities are essentially made of Cr and Fe (40 and 30 ppm, respectively) and are independent of the nitrogen content.

Green compacts were obtained by uniaxial and isostatic pressing at 50 MPa to form cylindrical pellets (20 mm in diameter and 8 mm height). The green density is obtained from the mass geometric dimensions of the disks and is kept constant at about 51±1% of the theoretical density. Organic binder (PVB 1 wt.%) is removed by a heat treatment in air at 450 °C.

The pellets were sintered in a graphite furnace under nitrogen static atmosphere (0.1 MPa); a powder bed composed of 75 wt.% 'MgAlON' and 25 wt.% BN is required to promote a stabilizing environment.[6] A secondary vacuum minimizes the oxygen partial pressure before introducing nitrogen. The temperature was increased at a heating rate of 10 °C/mn from 900 to the dwell temperature . Three different sintering temperatures (1650, 1750, 1850 °C) and five different dwell times were chosen (0; 2; 5; 8; 11; 14 h). The two extreme temperatures were associated with 5 and 11 h. The sample was finally cooled down in situ to room temperature. Tables 2 and 3 give the densification rate and grain size respectively, Fig. 1 shows some example of their polished and etched surfaces.

Table 3
Grain size of different samples

| Time (h) | | 0 | 2 | 5 | 8 | 11 | 14 |
|---|---|---|---|---|---|---|---|
| 1750 °C | A | | 12.0±7.0 | | 5.5±4.5 | | 7.0±5.0 |
| | B | | 8.0±5.0 | | 9±4.5 | | 9.5±5.0 |
| | C | | | | | | |
| | S30Cr | | | | 35±10 | | 40±25 |
| 1850 °C | A | 5.5±3.5 | | 12.0±7.0 | | 200±100 | |
| | B | 4.0±2.0 | | 10.0±5.0 | | 7.0±6.0 | |
| | C | 4.0±2.0 | | 11.5±6.0 | | 7.5±5.0 | |
| | S30Cr | 60±50 | | 45±20 | | 105±50 | |

### 2.2. Electrical breakdown tests

The breakdown phenomenon occurs when a dielectric material is submitted to a sufficient voltage to lead to the collapse of the insulating properties and the perforation of the sample. This intrinsic characteristic is considered to be a powerful parameter of the charge trapping ability of a material.

Insulating materials such as many ceramics can be characterized by their breakdown strength $E_b$ (kV/mm) obtained from the following relation:

$$E_b = \frac{V_b}{d}$$

$V_b$ is the breakdown voltage (kV) and $d$ the distance (mm) between the two electrodes (equivalent to the thickness of the sample).

The dielectrimeter used in this study (Dieltest DTS-BAUR) is operating on alternative current (50 Hz) at room temperature. The sample is soaked in a high voltage resistant oil bath ($60 < E_b < 80$ kV/mm) regenerated under vacuum after each series of tests The voltage rate is increasing at 1 kV/s until the breakdown occurs. The loss of insulating character is defined as a 3–4 mA current detected by the apparatus through the sample. Four samples for each composition and five tests on each sample are performed to evaluate the average breakdown strength $E_b$. A 5 mm distance between two successive impacts is required and considered to be enough to avoid electric interaction between two tests. Breakdown experiments are performed on 20 mm diameter cylindrical sample clamped between two

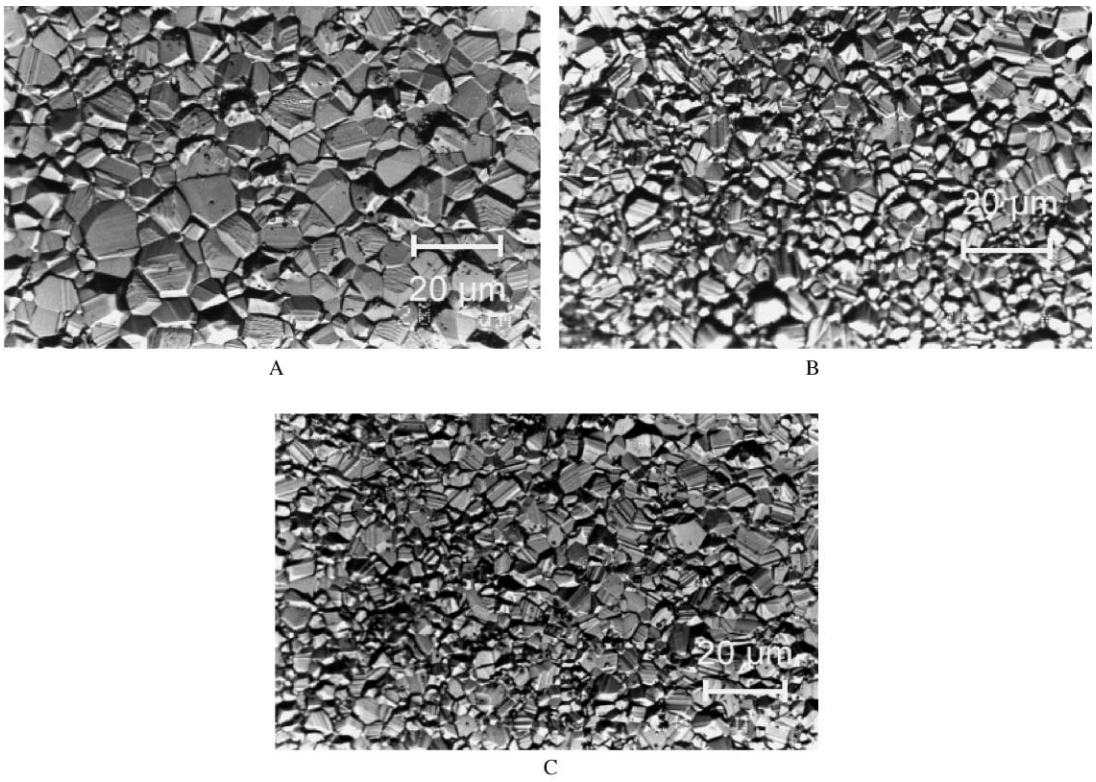


Fig. 1. Microstructures of A, B, C oxynitrides sintered 1850 °C—11 h.

hemispherical ended brass electrodes, the sample thickness is approximately 2.5 mm. All samples were tested after sintering to reduce surface contamination. A 1 min magnetic stirring of the oil bath is required after immersion of each sample in order to eliminate bubbles. The system is left quiet for 1 min to stabilize the environment of the sample before the voltage rises.

### 2.3. SEMME method

The charge trapping phenomenon of an insulating material can be experimentally estimated by way of an original technique called SEMME for 'scanning electron microscope mirror effect'.[7] The electron injection step on the sample is performed with a 30 kV focused electron beam, the surface of the sample excited by the irradiation is about 1 $\mu m^2$. As a result, negative trapped charges $Q$ are located on the upper face of the sample, which generate positive influence charges on the conductor holder. Consequently, an absorbed current $I_{ab}$ is measured between the holder and the ground, this current is directly proportional to the quantity of trapped charges by the relation:

$$\frac{dQ}{dt} = \alpha \times I_{ab}$$

where $\alpha$ ($\geqslant 1$) is a constant depending on both the geometric configuration of the device and the characteristics of the sample (thickness, dielectric constant).

The interpretation of the plots $I_{ab} = f(t)$ can give essential information about the mechanism of charge diffusion. Experimental data such as the maximum value of the absorbed current $I_{max}$ (first ms) or the decreasing shape of the curve $I_{ab} = f(t)$ can be also taken into account for the interpretation of the charge trapping phenomenon.

After the electron injection, a local electric field appears in the sample. When the surface of the sample is observed in scanning mode at low energy $V_I$, (from 100 V) the electron beam is deflected by the electric field, which acts as a mirror. The image of the SEM chamber can be then observed (Fig. 2).

The following electrostatic law leads to the calculation of the trapped charges )[7] $Q_p$

$$\frac{1}{d} = K \times \frac{V_I}{Q_p}$$

where

$V_I$ (V) is the acceleration voltage of the observation beam
$d$ (mm) is the diameter of the image of the last output diaphragm.
$K$ is a constant including the thickness and relative dielectric constant $\varepsilon_r$ of the sample and the geometric configuration of the set-up.

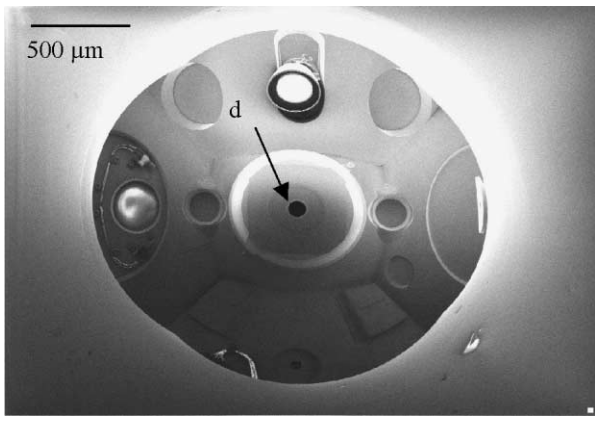


Fig. 2. Illustration of the 'mirror effect' by the SEM chamber observation.

The slope of the quasi-linear plot of $1/d$ versus $V_I$ is related to the quantity of trapped charges $Q_p$. The trapping yield $\pi = Q_p/Q_i$ ($Q_i$ being the quantity of injected charges), of the material for a given electron injection temperature can be then determined.

The detrapping potential is the observed potential for which the mirror vanishes.

## 3. Results and discussion

### 3.1. Electrical breakdown measurements

The three oxynitride and aluminate compounds were tested just after sintering, neither polishing nor annealing treatments were performed on these samples.

For the lowest isotherm (1650 °C), the breakdown strength values (Fig. 3) are ranging from 10 to 12 kV/mm for 5 and 11 h respectively. The standard deviation associated (graphically illustrated with error bars on each graph) is quite the same (roughly 1.5 kV/mm). The relative density is ranging from 70 to 75% of the theoretical density (TD) and is strongly influenced by the composition and the dwell time. Consequently we may suggest that, due to low heat treatment conditions, open porosity is widelydistributed in the sample and seem to govern the electrical breakdown phenomenon whatever the composition of the solid solution.

The intermediate isotherm (1750 °C) generates higher relative density ($94 < \rho/\rho_{th}(\%) < 98$) and so higher breakdown strength. The dwell time significantly influences $E_b$ values only for C sample and has no effect with A and B samples.

The 1850 °C isotherm leads to the highest relative density recorded in this study ($98 < \rho/\rho_{th}(\%) < 99$). The breakdown strengths associated exhibit also the highest values ($12.5 < E_b < 16$ kV/mm); however, a large deviation is recorded. The transition from 5 to 11 h is accompanied by an exaggerated grain growth for A sample (×20) and a slight decrease of $E_b$ values for both samples. Roles of both nitrogen and microstructure are very important for electrical breakdown behaviour.

The magnesium aluminate (Fig. 4) usually requires a lower sintering temperatures than that of 'MgAlON'

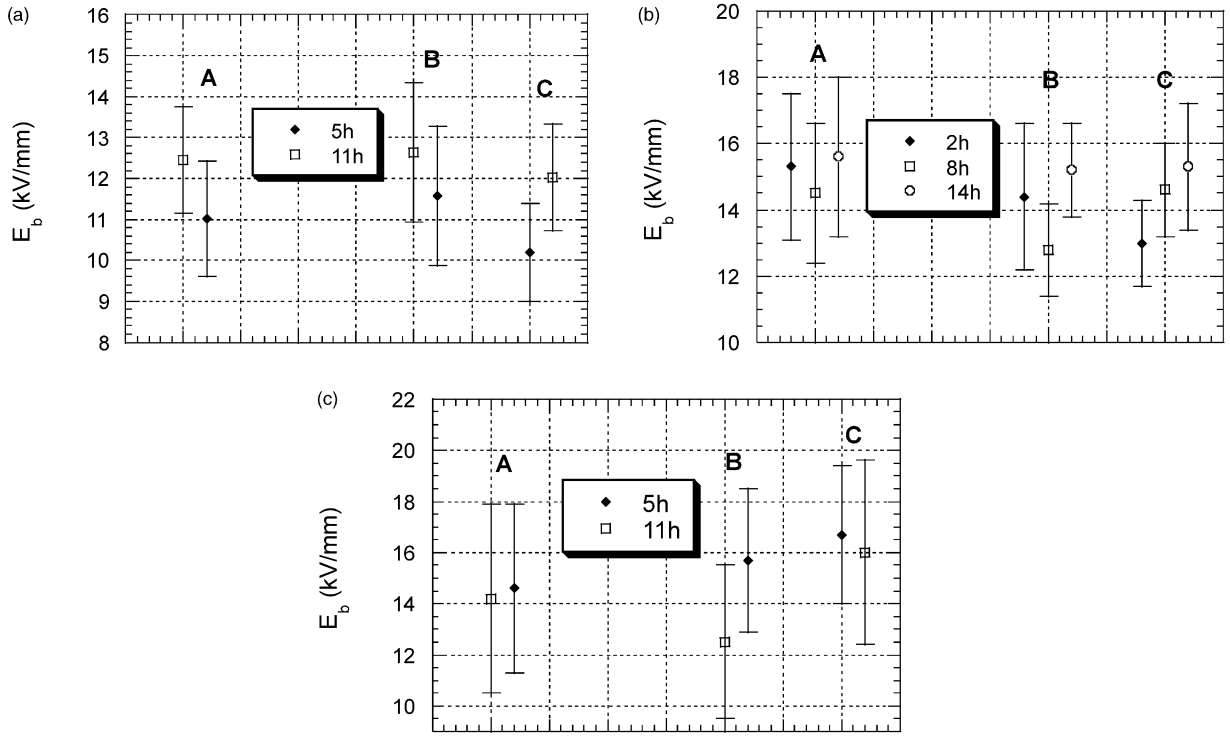


Fig. 3. Breakdown strength evolution for A, B and C samples according to the sintering temperature: (a) : $T = 1650$ °C, (b) : $T = 1750$ °C, (c) : $T = 1850$ °C.

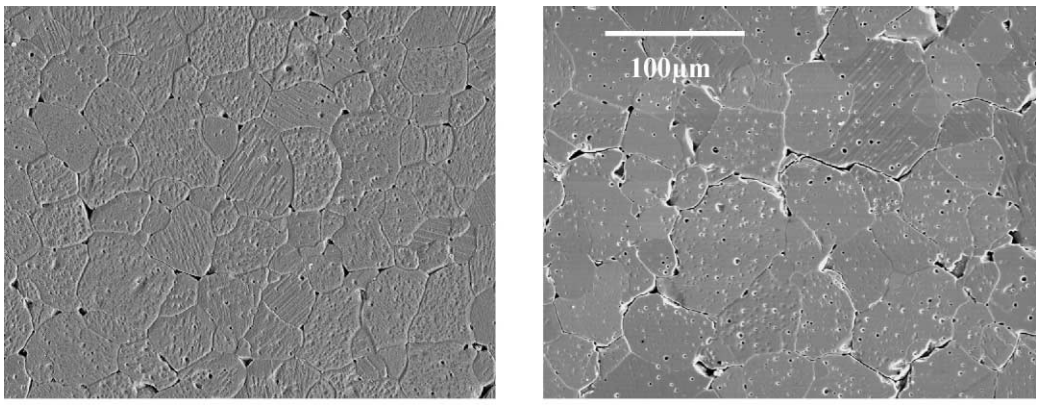


Fig. 4. SEM micrographs of $MgAl_2O_4$ samples sintered at (a): 1650 °C/5 h, (b): 1650 °C/11 h.

(typically 1500 °C under oxidizing atmosphere); however, the same heat treatment conditions ($T$, $t$, atmosphere) have been applied to S30Cr compound in order to make easier the comparison.

Fig. 5 summarises the breakdown strength of the $MgAl_2O_4$ reference: the general features are:

$E_b$ is slightly dependent on the dwell time at 1650 and 1750 °C.

$E_b$ strongly decreases when the sintering time is increased at 1850 °C due to exaggerated grain growth and dedensification (Tables 2 and 3).

The highest $E_b$ value (15 kV/mm) is quite similar to that obtained for A sample (14.5 kV/mm). Both are recorded at 1850 °C.

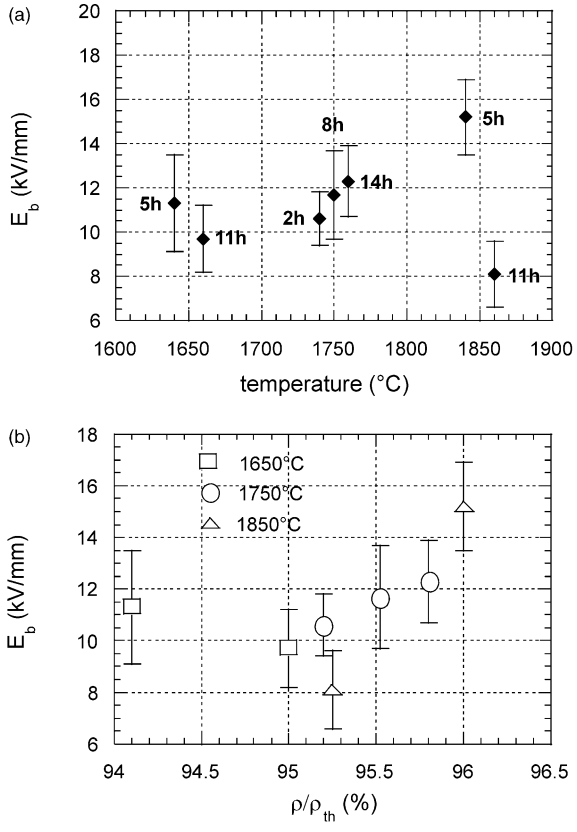


Fig. 5. Breakdown strength of $MgAl_2O_4$ sample versus (a): heat treatment conditions, (b): relative density.

The heat treatment at 1850 °C during 5 h leads to the highest breakdown strength for the four studied compositions. However, a large dispersion of values is obtained especially for 'MgAlON' samples. The presence of nitrogen limits the rate of densification of the sample and so the grain growth is less than that of the $MgAl_2O_4$ samples, the grain size is about 10 µm for samples with nitrogen, against 45 µm for the aluminate at 1850 °C—5 h. Moreover the microstructural parameter can be disregarded for 'MgAlON' compounds since the grain size ($\Phi \approx 10$ µm) is independent of the nitrogen content.

### 3.2. SEMME experiments

#### 3.2.1. The choice of observed samples by SEMME

The samples A,B,C heat treated at 1850 °C—5 h present the same microstructure ($d \approx 98.4\%$ and grain size $\approx 10$ µm). In these conditions, nitrogen-free samples present a densification value close to 96% and a grain size around 45 µm. Their electrical breakdown strength are $14.6 \pm 3.3$, $15.7 \pm 2.8$, $16 \pm 2.7$ and $15.3 \pm 1.9$ kV/mm respectively.

#### 3.2.2. Sample behaviour

All the experiments have been performed on a polished surface followed by a first heat treatment at 900 °C for 3 h under nitrogen atmosphere in order to reduce stresses induced during the polishing step. Before charge injection, the sample was annealed during 3 h under vacuum in the SEM chamber to minimize surface contamination. According to the device configuration, the temperature measured at the surface of the sample was about 70 °C though the set temperature was 300 °C,

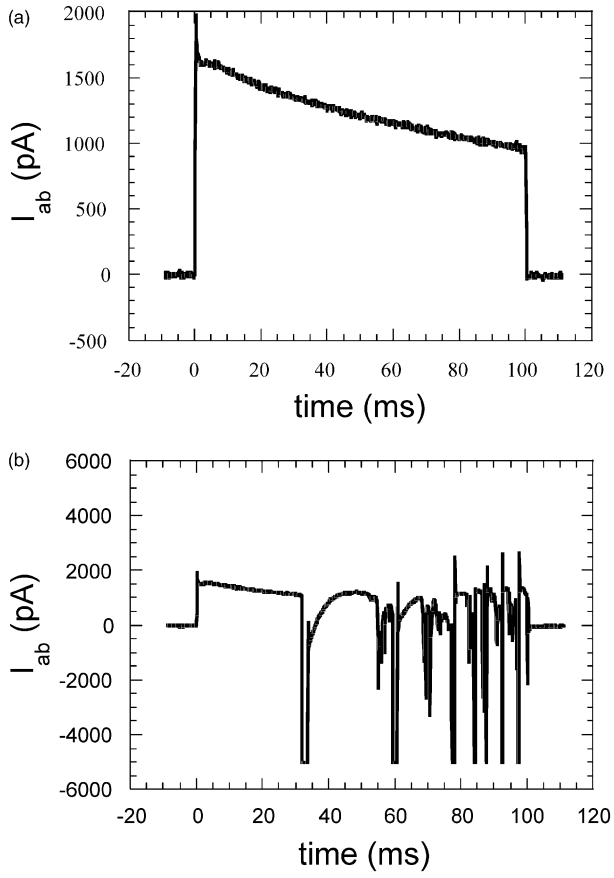


Fig. 6. Different cases of absorbed current variations versus injection time.

because of the bad thermal conductivity of the samples which are heated by contact with a heating-plate, and the vacuum of the microscope chamber . Afterwards, between two series of tests, each sample was annealed at 500 °C for 1 h under air to allow a complete evacuation of the implanted charges.

Conditions of charge injection have also to be optimised in order to observe a 'mirror effect'. The first series of experiments aimed at testing the reproducibility of the absorbed current curves versus the injection time. In this way, a statistical study has been conducted on the four samples. The conditions of electron injection at room temperature are set to a current of 3 nA during 100 ms which determine a quantity of injected charges $Q_i$ equivalent to 300 pC. Thus, 25 tests were performed on each sample. The curves $I_{ab}=f(t)$ obtained reveal two distinct behaviours as shown in Fig. 6.

The first case (Fig. 6a) is related to a high-absorbed current ($I_{max}\approx$2300 nA) at $t=t_o+\varepsilon$ corresponding to a great quantity of trapped electrons. These electrons located on the surface of the sample, at the injection point, act as an electronic barrier towards the next incident electrons, therefore the absorbed current curve decreases continuously during the injection time. This behaviour is always associated to mirror observation. The integral under the curve gives the quantity of trapped charges $Q_m$.

The second case (Fig. 6b) shows a first portion of the $I_{ab}=f(t)$ curve similar to the previous behaviour (same $I_{max}$ and decreasing slope) until a sudden collapse of the absorbed current occurs (at $t\approx$30 ms for this example) corresponding to a first electron reemission phenomenon. Afterwards, several oscillations can occurs as illustrated on Fig. 6b; as a result, this behaviour does not reveal a 'mirror effect'.

In these conditions of injection, the statistical study has indicated roughly 50% of both each cases except for B composition as mentioned in the Table 4.

The determination of the trapping yield could not be considered if electron reemission occurs, in this way the injection conditions might be optimised. For all samples a charge of 30 pC is accepted before the first reemission, so the new injection conditions will be $Q_i=30$ pC ($I_i=3$ nA, $t=10$ ms).

### 3.2.3. Relative dielectric constant $\varepsilon_r$

No data about the relative dielectric constant $\varepsilon_r$ of the 'MgAlON' compounds have been reported in the literature. Landolt and al. indicate a value of 7.7 for $MgAl_2O_4$.[8] As this parameter is included into the formula leading to the current calculation of the trapping yield $\pi$ (through the estimation of $Q_p$), an experimental determination of $\varepsilon_r$ has been made.The measure of the capacitance $C_P$ of the material for three different frequencies (100 Hz; 1 kHz; 1 MHz) allows a calculation of $\varepsilon_r$ since $\varepsilon_r$ is directly proportional to $C_P$ by the relation:

$$C_p = \varepsilon_o \times \varepsilon_r \times \frac{1}{k}$$

where $\varepsilon_0=8.854\ 10^{-14}$ F cm$^{-1}$; $1/k$ (cm) is defined as the ratio between the surface and the thickness of the sample.

This technique is accurate enough ($C_P\pm0.01$ pF) for dense materials ($d > 95\%d_{th}$).

All tested samples were coated with a 15 nm golden layer on both faces in order to optimise the contacts between the two electrodes and the material.

The reference $MgAl_2O_4$ shows a lower relative dielectric constant $\varepsilon_r$ value compared to 'MgAlON' compounds (≈20%). A slight nitrogen dependence of $\varepsilon_r$ is also recorded as mentioned by the values given in the

Table 4
Assessment of the statistical study for $Q_i=300$ pC

| | S30Cr | A | B | C |
|---|---|---|---|---|
| No electron re-emission (%) | 52 | 52 | 76 | 56 |
| Electron re-emission (%) | 48 | 48 | 24 | 44 |

Table 5
Experimental values of the relative dielectric constant $\varepsilon_r$

| | $d/d_{th}$ (%) | $\varepsilon_r$ (100 Hz) | $\varepsilon_r$ (1 kHz) | $\varepsilon_r$ (1 MHz) | $\varepsilon_r$ |
|---|---|---|---|---|---|
| A | 98.6 | 11.7 | 11.1 | 11.4 | 11.4 |
| B | 98.5 | 11.8 | 11.3 | 11.7 | 11.6 |
| C | 98.1 | 12.0 | 11.5 | 11.9 | 11.8 |
| S30Cr | 96.0 | 9.8 | 9.4 | 9.7 | 9.6 |

Table 5. Nevertheless, increasing the nitrogen content leads to a significant increase of $\varepsilon_r$, which should be interpreted as a local change of the lattice polarizability. This tendency has been already mentioned by Freer, on MgAlSiON glasses [9] where a linear dependence of $\varepsilon_r$ with nitrogen content was observed ($\varepsilon_r = 8$ for N≈15 wt). As the standard deviation does not exceed 5%, this parameter is considered to be independent of the frequency applied.

### 3.2.4. Trapping efficiency at room temperature

Several injections have been made on each sample to evaluate firstly the reproducibility of experiments. The results obtained are shown on Fig. 7.

Graphically, little differences are recorded from one composition to the other: $I_{max}$ is quite similar whatever the sample (≈2400 pA) and also the general shape of the decreasing curve. The interpolated slope at the first time of the decreasing curve indicates a higher value for the oxynitride compared to the reference oxide. However, this behaviour is minor and generates no significant variations of the trapped charges $Q_m$. A rapid decrease of the absorbed current can be interpreted as a low ability to diffuse charge in the material.

The previous evolutions of the absorbed current $I_{ab}$ versus injection time reveal an interesting dielectric feature, which might be completed by the observation of the 'mirror effect'. The charge trapped $Q_p$ is then experimentally determined from the linear electrostatic law (represented by the extrapolated line in the Fig. 8) and the trapping yield $\pi$ results of four experiments.

At room temperature, the trapping yield of the 4 compositions is large ($\pi \geqslant 83\%$) (Fig. 8). The detrapping potential is about 1 kV for the oxynitride and is slightly higher than the one observed on $MgAl_2O_4$ reference. This seems to indicate that a higher stability of the 'mirror', and therefore of the trapped charges, is obtained when nitrogen substitutes for oxygen in this spinel structure. This tendency has been observed at room temperature but gives no information about the efficiency of the traps at higher temperatures.

### 3.2.5. Trapping efficiency versus temperature

Experiments previously described have been performed at 33, 52, 77 and 90 °C). The thermal equilibrium between the SEM chamber and the surface of the sample is favoured by setting the temperature 24 h before the tests. We consider that the surface of the sample is in thermal equilibrium with the inside temperature of the SEM chamber. As a result, the thermal gradient can be considered as negligible.

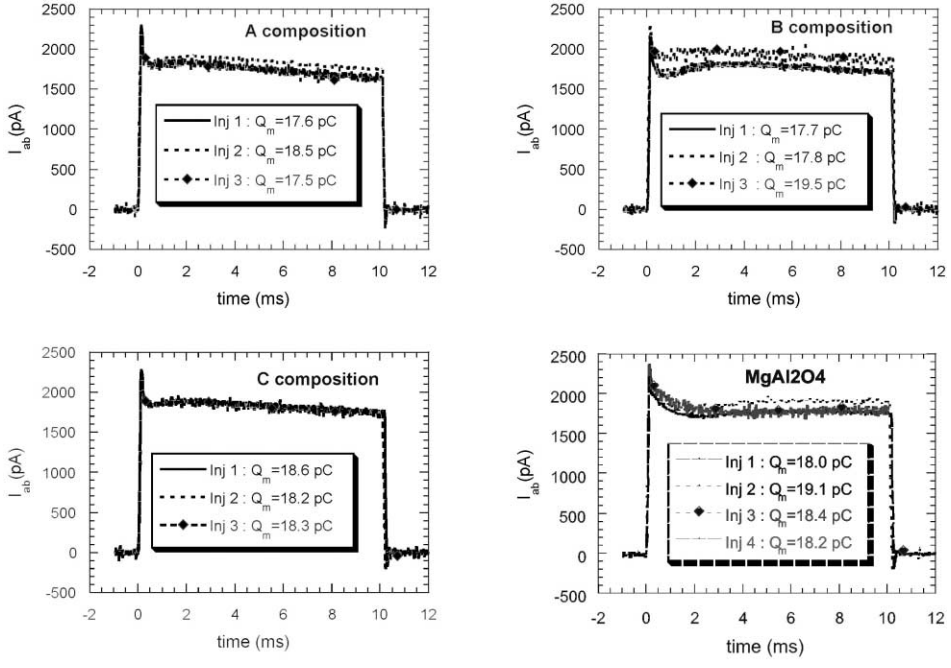


Fig. 7. Absorbed current curves at room temperature for the four compositions.

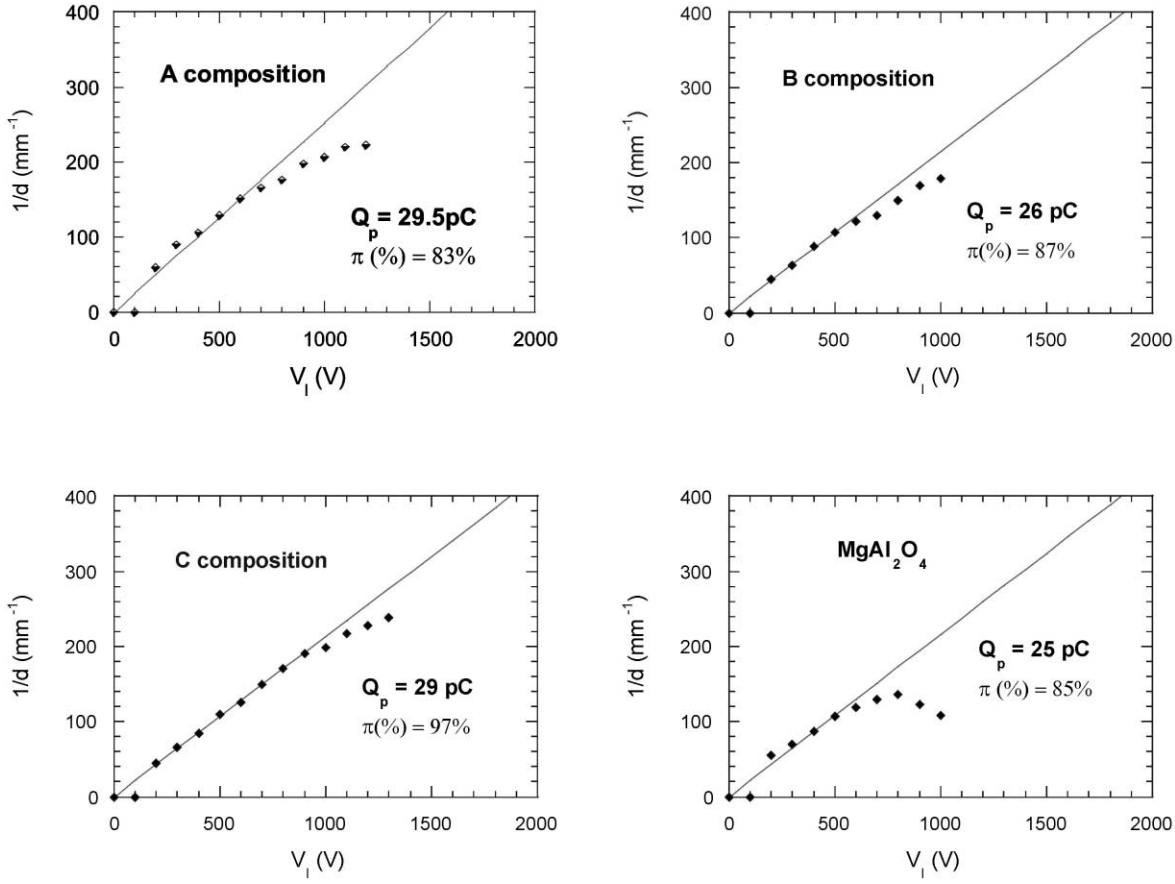


Fig. 8. Experimental determination of the trapping efficiency at room temperature.

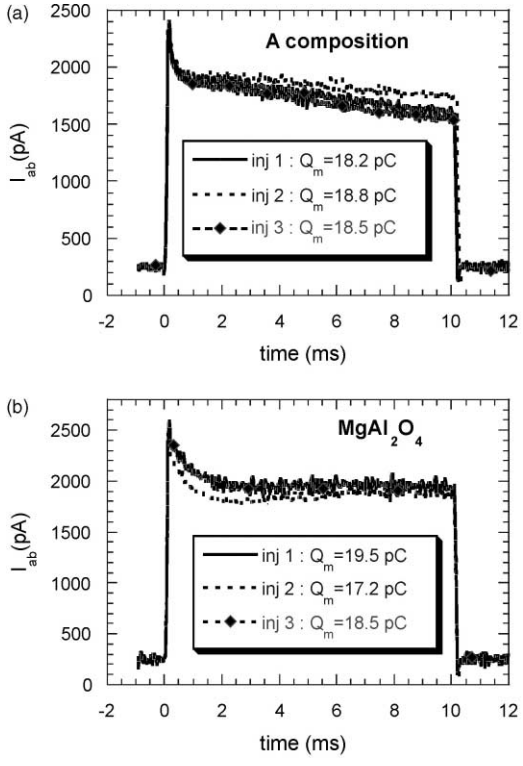


Fig. 9. Absorbed current curves for A compound and the reference oxide after injection at 90 °C.

The results about absorbed current, obtained for A and reference $MgAl_2O_4$ materials are shown on Fig. 9. Whatever the temperature used, the absorbed current curves $I_{ab}=f(t)$ remain quite similar. No electron reemission phenomenon has been observed. As a result, the trapping yield $\pi$ can be estimated for all samples and any temperature. Fig. 10 gives the evolution of $\pi$ versus the temperature of electron injection:

The general features are:

- The values of $\pi$ regularly decrease with the temperature
- The ranking previously established at room temperature is conserved in the range 20–90 °C.

The detrapping voltage is independent (≈1 kV) of the temperature, indicating a high stability of the charges trapped, even for high temperatures

The curves $\pi=f(T)$ could not be fitted by a Fermi Dirac function as proposed by Vallayer[10]. The inflexion point of this curve, also called the critical detrapping temperature $T_{CD}$, can give information about the depth of the trapping sites.

In order to estimate the nature and the quantity of point defects potentially able to play the role of charge

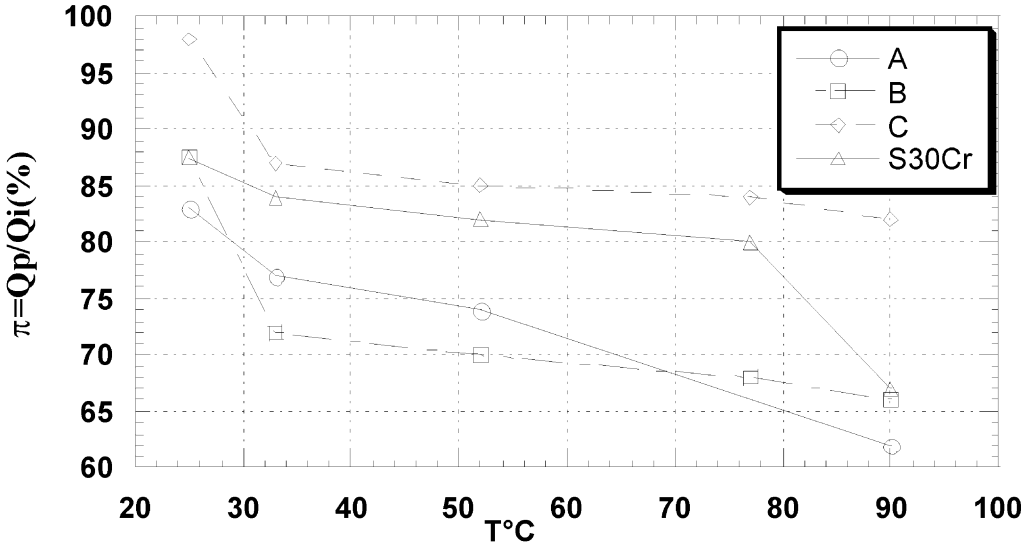


Fig. 10. Evolution of the trapping yield versus the temperature of electron injection.

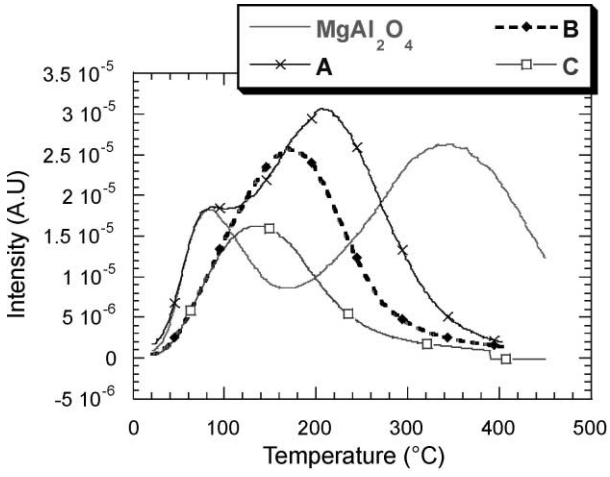


Fig. 11. TL spectra after UV irradiation.

traps, specific experiments based on spectroscopic techniques have been performed. Firstly after UV irradiation, thermoluminescent spectra of dense polycrystalline materials reveal the same features as are observed on the starting powders (Fig. 11).

A previous study on powder[3,5] has revealed the presence of a unique low temperature peak for 'MgAlON' compound identified as $Al_{Mg}$ centre. However, a small• shoulder appears at high temperature for A sample.

The spectral repartition of the three oxynitride compounds is reported in Fig. 12. The same tendency is recorded on dense polycrystalline materials about the $Cr^{3+}$ emission at 700 nm when compared with powders.[3,5] For A sample a band around 340 nm is present and may be consider as emission band representative of Fcation centres which are anionic vacancies having trapped one electron and surrounded by $Mg^{2+}$ in substitution of $Al^{3+}$;[11] it is consistent with its chemical formulation which permits a cationic inversion ($^{27}Al$ NMR experiments).[3,4] All oxynitride samples exhibit also a large emission band located around 450 nm (Fig. 12d). This emission band vanishes around 170 °C. Springis et al.[11] have mentioned a 410 nm emission on a single crystal of alumina which was ascribed to oxygen vacancies (denoted F centre). These defects, electrically neutral appear after the capture of two electrons according to the following mechanism :

$$F^{2+} + 2e^- \rightarrow F + h\upsilon \text{ with } \lambda = 450 \text{ nm}.$$

We may suggest that the sintering conditions of 'MgAlON' generate a large quantity of oxygen vacancies potentially able to trap electrons. In the one hand, the thermoluminescence (TL) curves of 'MgAlON' compounds indicate that the electron traps ($Al_{Mg}$•) are inactive after 400 °C and OMA (optical multichannel analysis) shows that the detrapping of electron from anionic vacancies (centre F), for C samples was made at 140 °C instead of 170 °C for A and B samples. In the other hand, the trapping yield at 90 °C, revealed by SEMME experiments, (about 80%) for C samples is much better than those of A, B samples (about 60%). These different results are not consistent between them. So, in MgAlON samples, electrons can be trapped by defect points particularly as $Al_{Mg}$• or $F^{2+}$ centres. But the good behaviour of rich nitrogen sample (C sample) may be understood also by the presence of heterogeneous zones randomly located as $AlN_4$ clusters which was shown in a previous work.[3,4] We suggest that these $AlN_4$ clusters significantly contribute to improve the mechanism of charge trapping in 'MgAlON' compounds by modifying the local polarizability of the lattice.

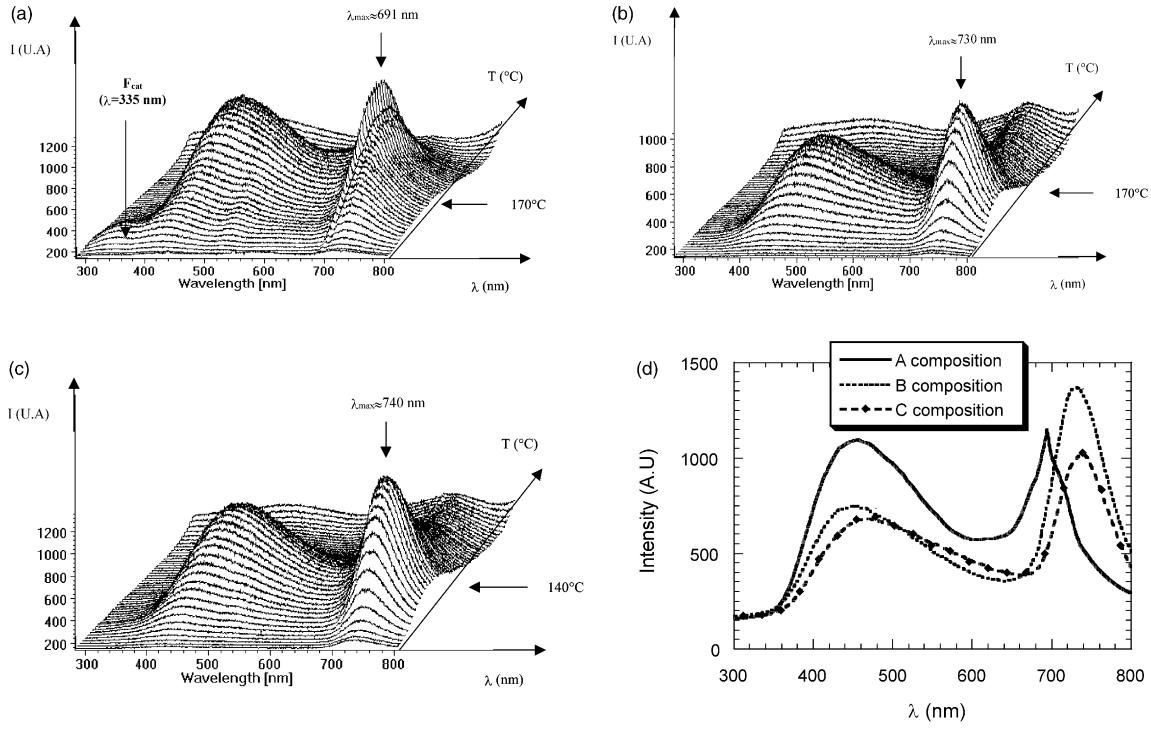


Fig. 12. OMA spectra after UV irradiation performed on (b) A; (b) B; (c) C compositions; (d) 2D spectra of A, B and C.

## 4. Conclusion

The breakdown strength behaviour of 'MgAlON' compounds has been investigated: a slight benefit effect of the composition was observed.

The SEMME experiments contribute to considerably improve the knowledge about the 'MgAlON' spinel solid solution:

- The absorbed current curves are not strongly influenced by either the composition or microstructure of 'MgAlON'. Thus, grain boundary density does not appear as a major parameter of the charge diffusion mechanism.
- The effect of composition is more effective on the trapping yield of 'MgAlON' as indicated by the values of $\pi$ obtained in the range 20–90 °C.

Subsequently, correlation between the charge trapping ability and the nature of point defects in 'MgAlON' solid solutions cannot be proposed. Oxynitrides trapping yield cannot be explained only by a few oxygen vacancies. So, on the basis of $^{27}$Al NMR results[3,4] we suggest that the evolution of the charge trapping behaviour is consistent with the existence of an electrically heterogeneous area induced by the presence of $AlN_4$·'MgAlON' compounds, especially for high nitrogen content (composition C) for which $AlN_4$ is increasing, are characterised by a high trapping yield even at 90 °C, by comparison with other insulating materials. For example, the trapping yield of a PSZ polycrystalline material is 40% at room temperature [12] when for an α-alumina single crystal it is about 80% at temperatures lower than −30 °C.[13] As a result, the 'MgAlON' solid solutions offer interesting properties for insulating applications.

## Acknowledgements

The authors would like to thank P. Iacconi of the University of Nice-Sophia Antipolis for helpful discussions about thermoluninescence and also the Laboratory 'Génie Electrique' of INSA de Lyon for the impedance analyser equipment.

## References

1. Blaise, G., Space charge physics and the breakdown process. *J. Appl. Phys.*, 1995, **77**, 2916–2927.
2. Miller, H. C., Flashover of insulators in vacuum. *IEEE Trans. Elec. Insul.*, 1993, **28** (4), 512–527.
3. Morey, O., *Rôle de l'Azote sur l'Élaboration et les Propriétés Diélectriques de Solutions Solides Spinelles de Type "MgAlON"*. Thesis St-Etienne, 2000.
4. Morey, O., Goeuriot, P. and Silly, G., 'MgAlON' spinel structure: a new crystallographic model of solid solution as suggested by 27Al solid state NMR. *J. Phys. Cond. Mater.* (submitted).
5. Morey, O., Goeuriot, P., Grosseau, P., Guilhot, B., Benabdesselam, M. and Iacconi, P., Spectroscopic analysis of 'MgAlON' spinel powders: influence of nitrogen content. *Solid State Ionics* (submitted).

6. Granon, A., Goeuriot, P., Thevenot, F., Guyader, J., L'Haridon, P. and Verdier, Y. Reactivity in $Al_2O_3$–AlN–MgO system. The MgAlON spinel phase. *J Eur. Ceram. Soc*., 1994, **13**, 365–370;
Liebault, J., Vallayer, J., Goeuriot, D., Treheux, D. and Thevenot, F., How the trapping of charges can justify the dielectric breakdown performances of alumina ceramics. *J Eur. Ceram. Soc.,* 2001, **21**, 389–397.
7. Vallayer, B., Blaise, G. and Tréheux, D., Space charge measurement in a dielectric material after irradiation with a 31kV electron beam: application to single-crystals oxide trapping properties. *Rev. Sci. Inst*., 1999, **70** (7), 3102–3112.
8. Landolt, H. and Bornstein, R. Numerical data and functional relationships in science and technology, ed. K. H. Hellwege. New Series, Berlin, Springer, 1980.
9. Freer, R. and Owate, I. O., *The Dielectric Properties of Nitrides, The Physics and Chemistry of Carbides, Nitrides and Borides*, 1990, pp. 639–651.
10. Vallayer, B., Blaise, G. and Treheux, D., Space charge measurement in a dielectric material after irradiation with a 30 kV electron beam. *Review of Scientific Instruments*, 1999, **70**, 3102–3112.
11. Springis, M. J. and Vallis, J. A., Visible luminescence of color center in sapphire. *Phys. Stat. Sol.(b)*, 1984, **123**, 335.
12. Medevielle, A., Thevenot, F. and Tréheux, D., Wear resistance of zirconias. Dielectrical approach. *Wear*, 1997, **213**, 13–20.
13. Bigarré, J., *Effet des Impuretés sur la Charge d'Espace dans l'Alumine. Application au Frottement*. Thesis, Ecole Centrale de Lyon, 1996.